Geological Society of America
Special Paper 418
2007

Slab disruption, mantle circulation, and the opening of the Tyrrhenian basins

Claudio Faccenna*
Francesca Funiciello
Dipartimento di Scienze Geologiche, Università Roma TRE, L. go S. Leonardo Murialdo 1, Rome, Italy

Lucia Civetta
Dipartimento di Scienze Fisiche, Università Federico II, Via Cinthia, Napoli, Italy, and
Istituto Nazionale di Geofisica e Vulcanologia, Osservatorio Vesuviano, Via Diocleziano 328, Napoli, Italy

Massimo D'Antonio
Istituto Nazionale di Geofisica e Vulcanologia, Osservatorio Vesuviano, Via Diocleziano 328, Napoli, Italy, and
Dipartimento di Scienze della Terra, Università Federico II, L. go S. Marcellino 10, Napoli, Italy

Monica Moroni
Dipartimento di Idraulica, Trasporti e Strade, Università di Roma "La Sapienza," Via Eudossiana 18, 00184 Rome, Italy

Claudia Piromallo
Istituto Nazionale di Geofisica e Vulcanologia, Via di Vigna Murata 605, 00143 Rome, Italy

ABSTRACT

Plate tectonic history, geological, geochemical (element and isotope ratios), and seismological (P-wave tomography and SKS splitting) data are combined with laboratory modeling to present a three-dimensional reconstruction of the subduction history of the central Mediterranean subduction. We find that the dynamic evolution of the Calabrian slab is characterized by a strong episodicity revealed also by the discrete opening of the Tyrrhenian Sea. The Calabrian slab has been progressively disrupted by means of mechanical and thermal erosion leading to the formation of large windows, both in the southern Tyrrhenian Sea and in the southern Apennines. Windows at lateral slab edges have caused a dramatic reorganization of mantle convection, permitting inflow of subslab mantle material and causing a complicated pattern of magmatism in the Tyrrhenian region, with coexisting K- and Na-alkaline igneous rocks. Rapid, intermittent avalanches of large amounts of lithospheric material at slab edges progressively reduced the lateral length of the Calabrian slab to a narrow (200 km) slab plunging down into the mantle and enhancing the end of the subduction process.

Keywords: subduction, Mediterranean, laboratory experiments, seismic tomography.

*E-mail: faccenna@uniroma3.it.

Faccenna, C., Funiciello, F., Civetta, L., D'Antonio, M., Moroni, M., and Piromallo, C., 2007, Slab disruption, mantle circulation, and the opening of the Tyrrhenian basins, *in* Beccaluva, L., Bianchini, G., and Wilson, M., eds., Cenozoic Volcanism in the Mediterranean Area: Geological Society of America Special Paper 418, p. 153–169, doi: 10.1130/2007.2418(08).

INTRODUCTION

Subduction-related magmatism is due to the fluids released by the dehydration and sometimes melting of the subducting crust (Tatsumi, 1986; Davies and Stevenson, 1992). This mechanism determines the location of the volcanic arcs, which are usually positioned on top of the 150 ± 50 km contour line of the Wadati-Benioff zones, and provides an explanation of the chemical and isotopic signatures of arc magmas. In the narrow regions wedged between the subducting slab and the upper plate, a convection cell operates by returning the flow produced by the shear coupling between the mantle and the subducting plate (Tovish et al., 1978). The shape and geometry of the convecting cell can be well established in two-dimensions (2-D; Tovish et al., 1978; Davies and Stevenson, 1992; Fischer et al., 2000; Conder et al., 2002; Eberle et al., 2002). In the Tonga subduction zone, the velocity of the return flow has been estimated to be in the order of 20%–30% of the subduction velocity (Turner and Hawkesworth, 1998). In Tonga, as in the South Sandwich and in the Kamchatka-Aleutian junction, geochemical data also suggest that the mantle wedge can be contaminated by both the melting of the slab at its edge or by the asthenospheric inflow of subslab mantle material turning around the slab (Wendt et al., 1997; Pearce et al., 2001; Yogodzinski et al., 2001; Leat et al., 2004). Moreover, examples of anomalous magma signature with respect to other volcanic arcs, including adakites, boninites and alkaline magmas (De Long et al., 1975; Gvirtzman and Nur, 1999; Doglioni et al., 2001; Yogodzinski et al., 2001; Deschamps and Lallemand, 2003) confirm the presence of slab windows where decompressional melting and asthenospheric inflow has generated pulses of mafic volcanism. Shear wave splitting below the Andean and other slabs, for example, illustrates a trench-parallel fast direction, which is usually interpreted as having been generated by the pressure produced by the retrograde motion of the slab (Russo and Silver, 1994). At slab edges (Tonga, Kamchatka, Sandwich), trench-normal fast direction, conversely, has been related to lateral return flow around the edge of the slab (Muller, 2001; Peyton et al., 2001; Smith et al., 2001; Leat et al., 2004). Under these conditions, the 2-D approximation is not appropriate because flow in the subduction wedge is far more complicated than expected. Recent laboratory models confirm these expectations (Funiciello et al., 2003; Kincaid and Griffiths, 2003; Funiciello et al., 2004a).

The Tyrrhenian Basin (Fig. 1A) represents a suitable test site to analyze the pattern of convection around the slab. The presence of a narrow slab beneath Calabria is expected to produce a complex pattern of mantle circulation and, in turn, a complex magmatic imprinting.

Here, we combine tectonic reconstruction, geochemical data (element and isotope ratio for younger than 800 ka volcanoes), and seismological data (P-wave tomography and seismic anisotropy) to constrain the way the mantle circulates around the deforming slab. We also highlight some simple physical aspects of three-dimensional (3-D) flow around a slab extracted from tank experiments. We conclude with a 3-D reconstruction of the slab during the last 10 m.y., which shows its progressive disruption with the formation of large windows that permit inflow of subslab mantle material and result in a complicated pattern of magmatism in the Tyrrhenian region.

TECTONIC CONSTRAINTS

Over the Cenozoic, Africa has been slowly converging toward stable Eurasia at ~1–2 cm/yr on average, on a NNE path until ca. 40 Ma, then on a northerly path, and finally rotating to a N20°W convergence (Dewey et al., 1989; Jolivet and Faccenna, 2000). This slow convergence has led to the build up of the Alpine chain in sites where continental collision (i.e., Adria versus Eurasia) has taken place. At ca. 30–20 Ma, the already slow convergence decreased (Silver et al., 1998; Jolivet and Faccenna, 2000). Although the precise paleogeographic configuration is still debated, a general agreement exists about the presence of a small Mesozoic oceanic basin that has facilitated, from 30 Ma onward, the retreat of the trench and the opening of the backarc basins (Le Pichon, 1982; Malinverno and Ryan, 1986).

As a consequence, extensional deformation is locally superimposed on sites of previous continental thickening, producing the disruption of the Alpine belt (Alvarez et al., 1974; Horvath and Berckhermer, 1982). In the land-locked environment of the Mediterranean oceanic basin, the progressive consumption leads to the progressive decrease of the size of the subducted plate. Presently (Figs. 1A and 2), the remnant of the subducted ocean lies mostly in the mantle, and subduction is still active only in small portions of the Hellenic trench and below Calabria, where a few hundreds of kilometers are still available for subduction.

The evolution of the Calabrian slab and its retreat, in particular, is rather impressive because, in a restricted area, the trench rolled back for more than 800 km, inducing the opening of new small oceanic basins. The first episode of the backarc extensional process led to the opening of the Liguro-Provençal Basin. The age of the synrift and postrift deposits (Cherchi and Montandert, 1982; Burrus, 1984; Gorini et al., 1994; Seranne, 1999) indicates that the initial phase of stretching lasted from 30 to 21 Ma before lithospheric break-up and oceanic spreading occurred (21–16 Ma), while the Sardinia-Corsica block rotated counterclockwise (van der Voo, 1993; Speranza, 1999). Along a NE-SW cross section, running from the Gulf of Lyon to Calabria (Fig. 1B), estimates of oceanic spreading range from 150 km (Mauffret et al., 1995) to 190 km (Faccenna et al., 2001a) to 230 ± 20 km (Burrus, 1984; Chamot-Rooke et al., 1999), while rifting ranges from 150 ± 20 km (Chamot-Rooke et al., 1999) to 200 km (Faccenna et al., 2001b). Backarc extension was accompanied by the growth of a well-developed volcanic basaltic-andesitic arc, which erupted along the Sardinia-Provençal margins (Beccaluva et al., 1989, 1994, 2005a, and references therein) from 32–34 Ma to 13 Ma (Fig. 1B). The subduction zone during this phase extended from northern Tunisia to the Maghrebides and to the Apennines, but its westward lateral prosecution is still debated because it is related

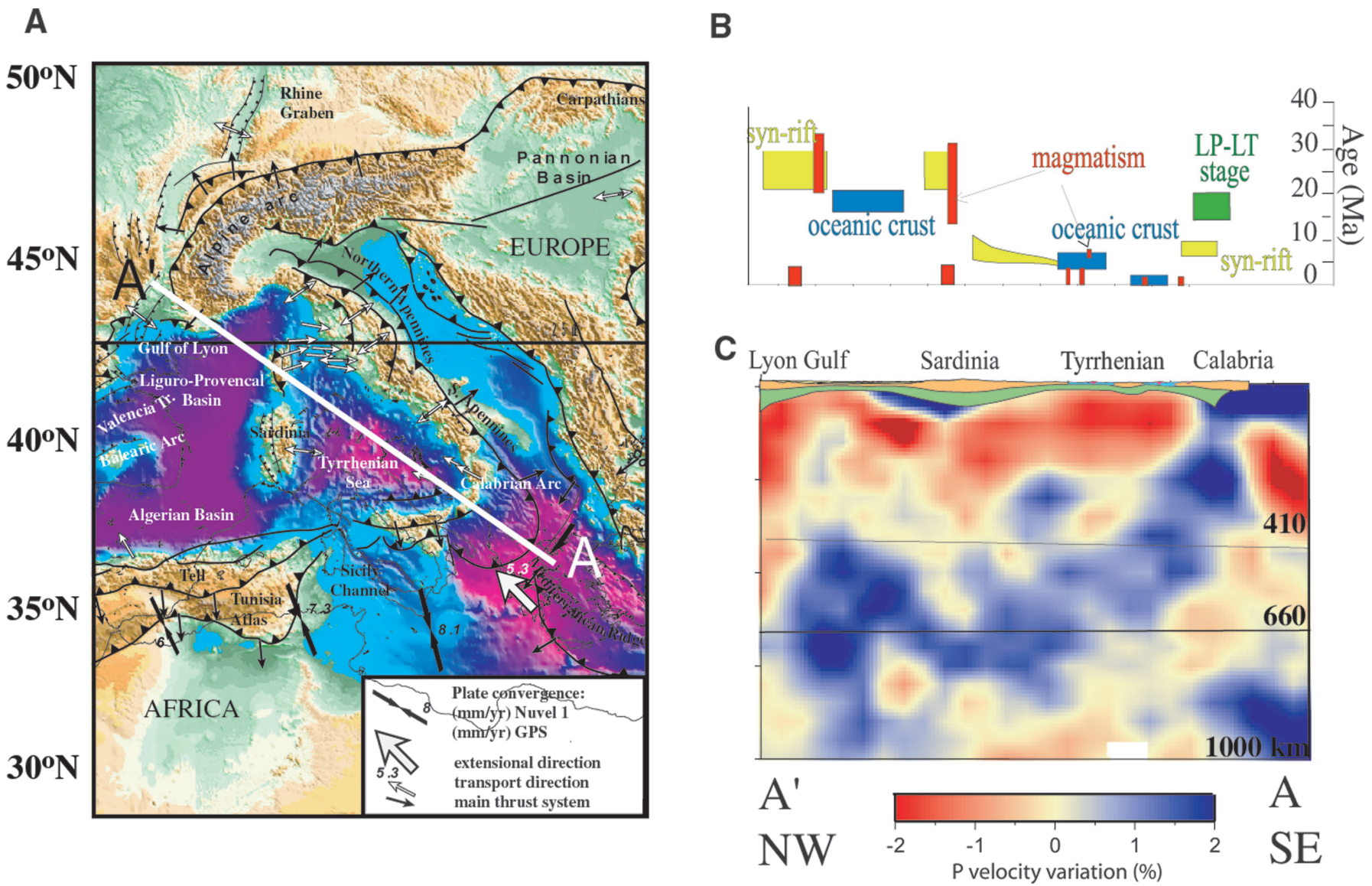

Figure 1. Present-day tectonic framework and deep structure of the central Mediterranean region. (A) Topography and tectonic features. The white A–A′ line indicates the reference section running from the Gulf of Lyon to Calabria. (B) Age of rifting or spreading phases (backarc extension), magmatism, and low-pressure–low-temperature (LP-LT) stage of metamorphism (see text for references). (C) Lithospheric cross section and tomography model along the reference section A–A′ (from Piromallo and Morelli, 2003). Lithospheric and crustal data are after Chamot-Rooke et al. (1999) and Jolivet and Faccenna (2000).

Figure 2. Tectonic map of the southern Tyrrhenian Sea showing subduction-related and intraplate volcanism. Dashed lines show the isobaths (km) of the Wadati-Benioff zone.

to the age of the contiguous Algerian Basin. Some reconstructions have proposed that the Algerian Basin opened in the same time interval of that of the Liguro-Provençal Basin (Verges and Sabat, 1999), while some others have proposed a younger age between 16 and 8 Ma (Roca et al., 1999; Faccenna et al., 2001b; Mauffret et al., 2004). Following the latter reconstruction (see Faccenna et al., 2004, for discussion), the subduction zone should have reached a sharp bend, and probably a lateral tear of the slab, just south of Sardinia (Fig. 3A). The opening of the Tyrrhenian Basin occurred after a small pause of extension and magmatism, lasting ~3–5 m.y., when extension and magmatism virtually ceased (Fig. 3). The age of the first extensional-related deposits in the Tyrrhenian Basin shoulder is probably Tortonian (Sartori et al., 2001), although Serravallian extension-related deposits have been described in Calabria (Mattei et al., 2002). Vigorous extension and subsidence, however, took place during the Tortonian and got progressively younger (10 Ma to 5 Ma) from the Sardinia margin toward the Vavilov Basin (Wezel et al., 1981; Kastens et al., 1988; Sartori and Staff, 1989; Spadini and Podladchikov, 1996). Oceanic spreading in the Tyrrhenian occurred in two distinct episodes. The first oceanic center formed during the Pliocene in the Vavilov Basin (4–3 Ma; Fig. 3B). The second one occurred further to the east into the Marsili Basin (Fig. 3C), which shows activity younger than 2 Ma, and which probably ceased before 1 Ma, restricting its activity to the growth of the Marsili seamount (Marani and Trua, 2002; Nicolosi et al., 2006). The pulsating eastward shift of the locus of accretion was also accompanied by a decrease in the length of the accreting basin, indicating a decrease in the active pulling portion of the subducting lithosphere. The total amount of extension in the Tyrrhenian evaluated by Malinverno and Ryan (1986) is on the order of 330–350 km (Patacca et al., 1990; Spadini and Podladchikov, 1996; Faccenna et al., 2001b).

The episodes of the backarc basins are in good correspondence to the architecture of the outer thrust front as revealed by the age of the flexural-related deposits (Casero, 2005). In particular, the outer front appears to be punctuated by the cessation of compressional and flexural activity moving eastward from the African Tell to Calabria. First, in the Late Tortonian, the Tell ceased its activity (Casero and Roure, 1994). Then, the western edge of the active thrust front shifted again eastward ~300 km in the Messinian–early Pliocene, because of the cessation of the Sicily Channel fold-and-thrust belt (Argnani et al., 1987; Casero and Roure, 1994). Soon after, the inactive foreland thrust belt was cut by a NW-SE–trending rift system of the Sicily Channel (Figs. 1A and 2) (e.g., Argnani, 1990). The present-day shape of the arc should have been attained at that time because significant counterclockwise rotation of the southern Apennines (25° according to Sagnotti, 1992, and Scheepers et al., 1993), in fact, occurred between the early Pleistocene and the middle Pleistocene (Mattei et al., 2004), while the Calabrian region itself rotated clockwise of ~15°–25° during the Pliocene-Pleistocene (Scheepers et al., 1993; Scheepers and Langereis, 1994; Speranza et al., 2000). Finally, the southern Sicily thrust system (Gela nappe) ceased to

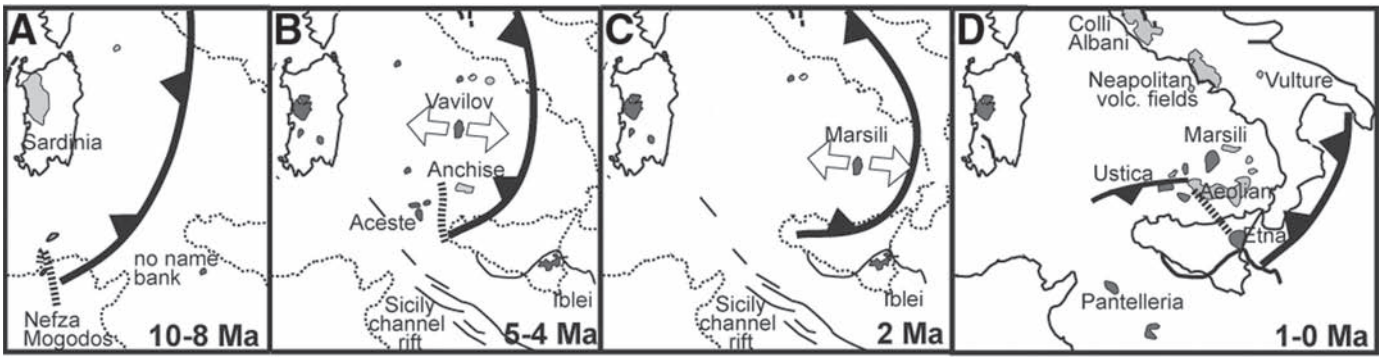

Figure 3. Tectonic reconstruction of the evolution of subduction and backarc extension in the central Mediterranean (from Faccenna et al., 2004). Four crucial phases are shown: (A) 10–8 Ma; (B) 5–4 Ma; (C) 2 Ma; and (D) 1–0 Ma. Dashed lines indicate the lateral boundary between subduction-related and anorogenic volcanism.

be active at around 800 ka (Argnani et al., 1987), restricting the present-day configuration of the active front to the Ionian area. Similarly, the southern Apennines thrust belt also decreased its activity dramatically around 0.8–0.7 Ma (Patacca et al., 1990; Mattei et al., 2004), although, locally, in its more external portion, it appears not to have completely vanished (Doglioni et al., 1999; Bertotti et al., 2001). The space-time eastward punctuated shift of the flexural portion of the thrust belt indicates an along-strike segmentation of the subducted lithosphere moving eastward from the African to the active portion of the Calabrian slab (Casero and Roure, 1994).

The segmentation of the subducted lithosphere is also indicated by the nature of volcanism as alkaline anorogenic volcanism supplants the calc-alkaline type invading the southern Tyrrhenian region. First, by the late Miocene (ca. 8–6 Ma) in northern Tunisia, the calc-alkaline rhyolite suites of Nefza and Galite Islands (14–8 Ma; Savelli, 2002) were replaced with the (Na)-alkaline basalt of Nefza and Mogods (Fig. 2). Then, to the north of the Sicily Channel region, the alkaline Aceste seamount was emplaced just west of the calc-alkaline Anchise seamount during the early Pliocene, and anorogenic alkaline magmatism started its activity in Sardinia (Savelli, 2002; Beccaluva et al., 2005b). Finally, around the early Pleistocene, Ustica volcano and Prometeo lava field, located just to the west of the Aeolian volcanic fields, erupted magmas with affinity similar to those erupted at Pantelleria and Linosa Islands (Cinque et al., 1988; Civetta et al., 1998; Trua et al., 2003; Fig. 2).

SEISMOLOGICAL CONSTRAINTS

The Calabrian arc is the only region of the Mediterranean where earthquakes are recorded all along an approximately continuous dipping plane from crustal (0–30 km) to deep upper-mantle depth. Seismicity is distributed along a narrow (~200 km) and steep (~70°) Wadati-Benioff plane, which strikes SW-NE and dips NW, down to ~500 km (e.g., Anderson and Jackson, 1987; Giardini and Velonà 1991; Selvaggi and Chiarabba, 1995). The presence of seismicity on a well-defined Wadati-Benioff zone reveals a direct trace of the past and still active process of lithospheric subduction from the Ionian foreland below the Calabrian arc and Tyrrhenian Sea.

The high-resolution, large-scale tomographic model PM0.5 (Piromallo and Morelli, 2003), obtained for the whole Euro-Mediterranean region through the inversion of the large data set of regional and teleseismic P-wave delay times by the International Seismological Centre (ISC), gives further constraints on the slab morphology. In Figure 4A, we show an enlargement of the model in the region of interest, the southern Tyrrhenian area, at two representative horizontal layers (200 and 500 km). The layer at 200 km depth roughly marks the limit between two depth ranges in which the seismic velocity of the region is characterized by a different structure. Below 200 km depth, the high-velocity anomaly that correlates to the Calabrian arc joins into a continuous belt with the southern Apennines to the north and with the Sicily-Maghrebides chain to the southwest (Faccenna et al., 2003; Piromallo and Morelli, 2003). Moving from 200 km depth to the surface, instead, high-velocity anomalies along the peninsula appear to be disconnected from each other and are interrupted by wide gaps of low-velocity anomalies (below the southern Apennines and the Sicily Channel). Therefore, the Calabrian arc is the only place where, along a segment which has a lateral extent that reaches ~200 km, the high-seismic-velocity structure, which we interpret as a cold subducted lithosphere, is vertically continuous all over the depth range, from the surface to the transition zone. The map at 500 km depth, located in the middle of the transition zone (Fig. 4A), shows another representative layer, in which we can clearly see how the Calabrian fast anomaly merges into a broader positive anomaly, which spreads all over central Europe and the western Mediterranean. This large-scale, high-velocity anomaly, which characterizes the transition zone (Piromallo and Morelli, 2003), probably gathers the material from different slabs. Below the western Mediterranean, we find the traces of Betic-Alboran, Algerian, Apenninic, and Calabrian slabs (Carminati et al., 1998; Wortel and Spakman, 2000; Faccenna et al., 2003), while below central Europe, fast velocity material likely comes from the Alpine-Carpathians subduction (Wortel and Spakman, 2000; Piromallo and Faccenna, 2004).

The vertical profile A–A′ (Fig. 1C) crosscuts the positive anomaly of the Calabrian arc, approximately parallel to the direction of maximum extension of the Tyrrhenian Basin. The high-velocity structure can indeed be followed continuously, starting from a shallow horizontal portion, located on the Ionian side of the arc, which connects to a feature that deepens steeply to the NW into the mantle, down to 400 km, and then bends almost horizontal in the transition zone, where it lies on the 660 km discontinuity. Below the Tyrrhenian Basin, a low-velocity anomaly is detectable from the surface down to the top of the transition zone at 400 km, which is overlain by the fast shallow anomaly of the Sardinia-Corsica block. In the eastern portion of the cross section, note also the pronounced slow anomaly at intermediate depths, just behind the slab-like fast one.

Cross-section B–B′ (Fig. 5), which is orthogonal to the previous profile, intersects the Calabrian fast anomaly along-strike, imaging the slab as a trapezoidal structure and showing its limited lateral extent. On its left side, a very strong slow anomaly is located in the shallower 150 km below the Sicily Channel and western Sicily. On the top right side of the trapezoid, another pronounced slow anomaly is imaged, below the southern Apennines, as is, further to the east, the fast slab-like body deepening below the Hellenides.

The 3-D contour of the 0.8% high-seismic-velocity anomaly better illustrates the present-day shape of the Calabrian slab (Fig. 4B), which has been reduced to a narrow, finger-like, structure.

These large-scale features are consistent among recent tomographic studies at comparable upper-mantle scale and resolution (Wortel and Spakman, 2000; Piromallo and Morelli,

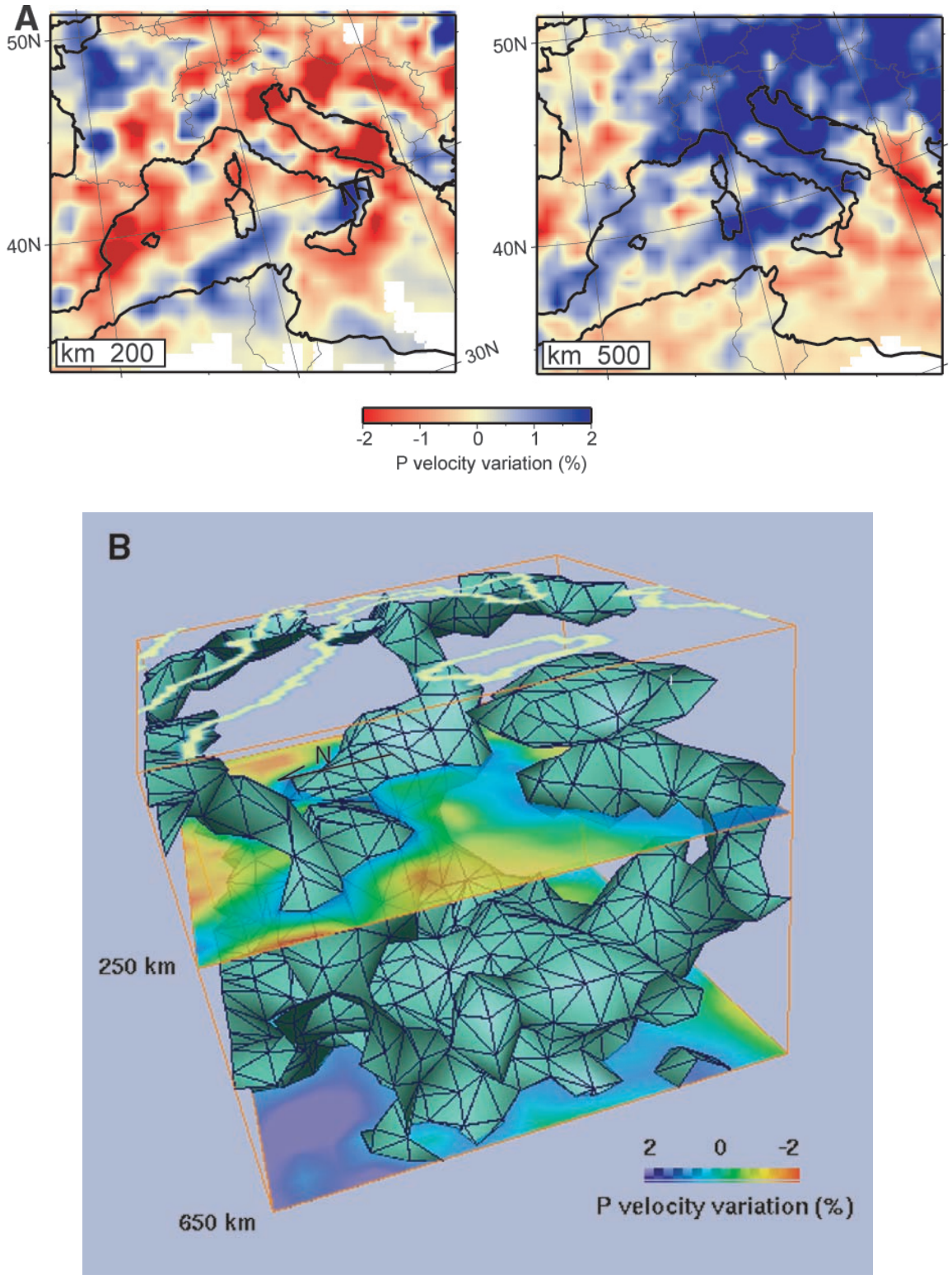

Figure 4. (A) Map views of tomographic results at 200 and 500 km depth from tomographic model PM0.5 (Piromallo and Morelli, 2003). Velocity anomalies are displayed in percentages with respect to the reference model *sp6* (Morelli and Dziewonski, 1993). (B) 3-D image of the mantle tomographic structure beneath the central Mediterranean (from Piromallo and Morelli, 2003). The green iso-surface represents seismic velocity anomalies larger than +0.8%. The layers at 250 and 650 km depth are shown in transparency as reference sections.

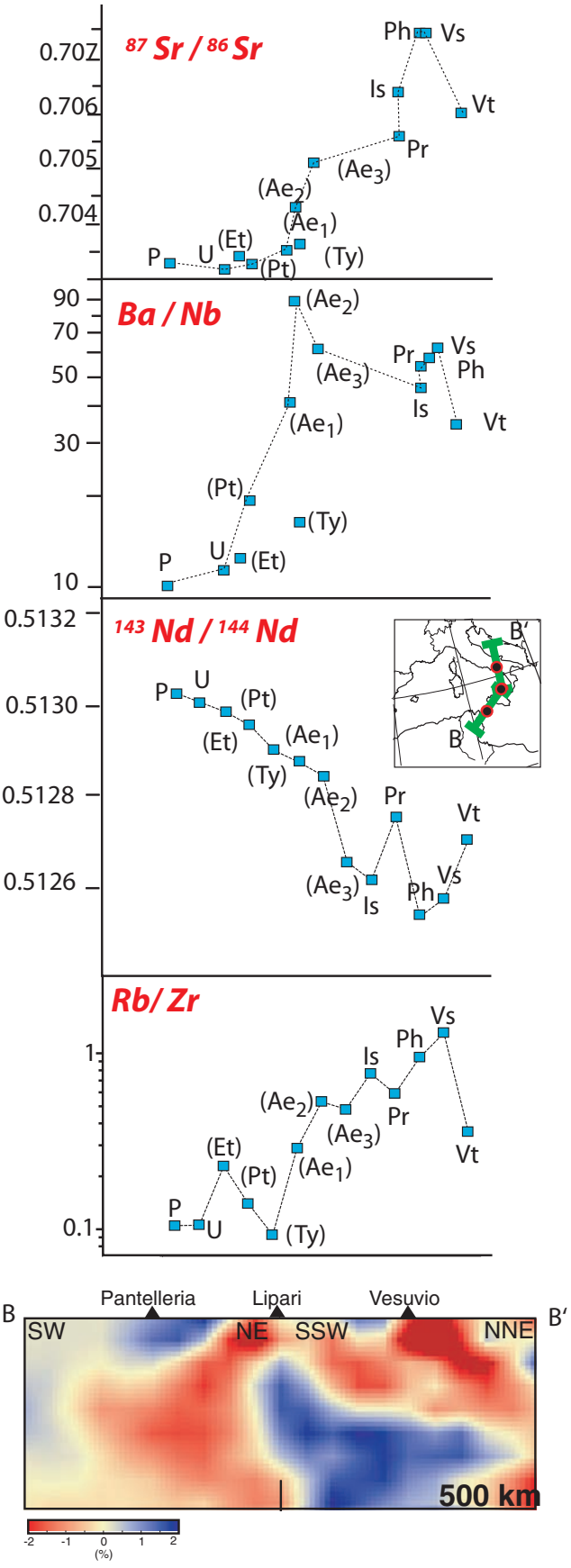

2003). The local scale teleseismic model by De Gori et al. (2001) gives instead a different picture, since the authors interpreted the detected velocity anomalies as a continuous slab below the southern Apennines, from 65 to 285 km depth, where larger-scale models image instead strongly negative (Piromallo and Morelli, 1997; Wortel and Spakman, 2000; Piromallo and Morelli, 2003) or close to zero (Lucente et al., 1999) velocity anomalies. Since the study by De Gori et al. (2001) samples a small inversion volume by teleseismic rays only, the resulting model is likely affected by vertical smearing, and high-velocity anomalies located beneath the bottom of the model can be erroneously mapped inside, thus hampering the detection of a vertical gap in the high-seismic-velocity structure.

Some authors (e.g., Carminati et al., 2005; Scrocca et al., 2005) have remarked that ~170 km and 280–300 km of continental lithosphere has gone into the subduction zone below the northern and southern Apennines, respectively, and that the compositional heterogeneities in the subducted lithosphere could be reflected in the observed seismic velocity anomalies. In their view, the negative velocity anomaly below the southern Apennines should not be interpreted as a slab window but rather as subduction of continental lithosphere. However, in that case, we would expect a similar seismic signature below the northern and southern sector of the chain, at least in the shallower portion (~150 km) where the same kind of lithosphere (continental) has entered subduction. In this depth range, instead, different tomographic models agree in giving a heterogeneous velocity structure along the chain, which conversely becomes more uniform at depths more than 200 km (e.g., Piromallo and Morelli, 1997; Lucente et al., 1999; Wortel and Spakman, 2000).

Figure 6 plots the pattern of SKS splitting measurements (Civello and Margheriti, 2004) in the southern Tyrrhenian Sea over the 150 km depth tomographic map. Anisotropy is defined by two parameters, fast direction (ϕ) and delay time (δt), which are related to lattice preferred orientation of olivine crystals induced by mantle deformation and/or flow. Shear wave splitting δt in the studied region ranges from 0.5 to 2.7 s; the average is ~1.6 s, which corresponds to about a 180-km-thick anisotropic body with ~5% anisotropy intensity. Fast directions in peninsular Italy are quite often parallel to the strike of the thrust belt, ranging from NW-SE in the Vesuvian area to NNE-SSW in eastern Sicily to EW in central Sicily. This pattern of seismic anisotropy along retreating subduction can be interpreted as being due to flow of

Figure 5. $^{87}Sr/^{86}Sr$, $^{143}Nd/^{144}Nd$, Ba/Nb, and Rb/Zr ratios (data compiled from the literature; see text for references) for key volcanoes of southern Italy active during the past 800 k.y. Pantelleria (P), Ustica (U), Prometeo (Pt), Aeolian islands (Ae1: Alicudi; Ae2: Filicudi + Salina + Vulcano + Lipari + Panarea; Ae3: Stromboli), Procida (Pr), Ischia (I), Campi Flegrei (CF), Somma-Vesuvius (Vs), Vulture (Vt). Data for Etna (E) and Tyrrhenian Sea mid-ocean-ridge basalt (MORB) (Ty) (Vavilov) are also projected on the profile. Data are presented on the profile B–B′ running from SW to NNE over the tomographic model (from Piromallo and Morelli, 2003).

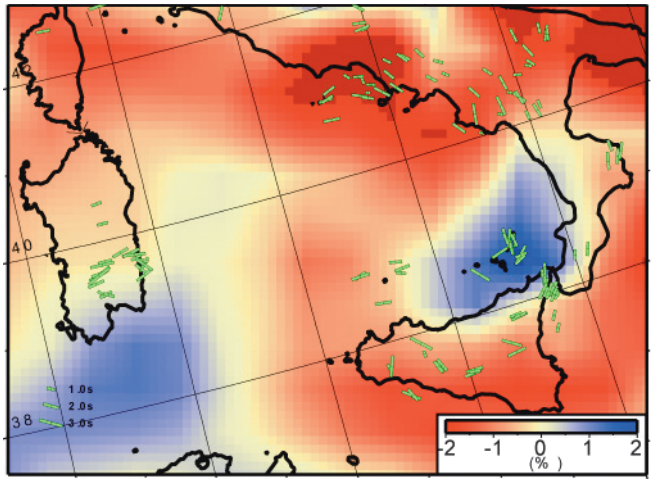

Figure 6. SKS wave splitting measurements in the Tyrrhenian region (from Civello and Margheriti, 2004). Measurements are represented by solid lines oriented parallel to ϕ with length proportional to δt. Measurements are plotted over the tomographic image (layer at 150 depth) at the surface projection of the 150-km-depth SKS ray piercing point. Fast directions are prevalently trench parallel below the slab and rotate to trench normal at the western edge of the slab, moving in a circular motion.

subslab mantle material produced by the overpressure related to the retrograde motion of the slab (see section title Mantle Circulation around a Slab: Laboratory Experiments).

Conversely, in the Tyrrhenian Sea, fast directions are mainly oriented E-W (Sardinia, Ventotene, and Ustica Island) and can be interpreted as having been induced by trench-suction, because they match the backarc extensional direction. The Aeolian Islands have a complex pattern of polarization, which is possibly related to slab deformation. The NS-oriented ϕ in western Sicily strikes at a high angle with respect to the thrust front and could be related to lateral return flow turning around the slab edge (see section Mantle Circulation around a Slab: Laboratory Experiments). The rather scattered ϕ in northwest Calabria, which ranges from N-S to E-W, is probably connected to the anisotropy of the slab itself.

GEOCHEMICAL CONSTRAINTS

Figures 1 and 2 show that the magmatism of the southern Tyrrhenian Sea is characterized by a close association of alkaline (sodic, potassic, ultrapotassic) and calc-alkaline products. In particular, Quaternary sodic alkaline basalts crop out on the islands of Pantelleria, Linosa, and Ustica, submarine Prometeo lava field, Etna, Iblei, and Vulture (Fig. 1). These volcanics are geochemically and isotopically akin to ocean-island basalts (OIB; e.g., Cinque et al., 1988; Beccaluva et al., 1998; Civetta et al., 1998; Beccaluva et al., 2002; Gasperini et al., 2002; Trua et al., 2003). Calc-alkaline volcanic activity has occurred at the Aeolian arc, and other seamounts in the Tyrrhenian Basin, such as Anchise and Aceste (e.g., Francalanci et al., 1993; Beccaluva et al., 1994; Del Moro et al., 1998; De Astis et al., 2000). In the Campanian region, ca. 2 Ma calc-alkaline lavas found in boreholes drilled in the Volturno Plain were followed by Quaternary K-alkaline magmas emitted by the Neapolitan volcanoes (Campi Flegrei, Ischia, Procida, Somma-Vesuvius). All these are genetically related to subduction processes occurring in the Tyrrhenian Basin (e.g., Di Girolamo et al., 1976; Beccaluva et al., 1991; D'Antonio et al., 1996, 1999; Peccerillo, 1999; Serri et al., 2001; Tonarini et al., 2004). Nevertheless, one fundamental question that remains unanswered is the significance of the close association in space and time of contrasting magmatic suites in the complex geodynamic context of the southern Tyrrhenian Sea (e.g., Ellam et al., 1989; Beccaluva et al., 1991, 2005a; Peccerillo, 1999; Serri et al., 2001; Schiano et al., 2004). Some hypotheses have been proposed that invoke the presence of either N-NW–directed African asthenospheric mantle flow or a vertical mantle plume rising through a slab tear/window that mixes with the upper part of subducted lithosphere (Gvirtzman and Nur, 1999; Doglioni et al., 2001; Gasperini et al., 2002; Trua et al., 2003); however, a general model that takes into account all the geophysical, petrological, and geological data is still lacking.

It is widely accepted that geochemical and isotopic tracers can provide useful information for mapping mantle structures (e.g., Pearce, 1982). To evaluate the mantle composition (i.e., orogenic versus anorogenic) in the southern Tyrrhenian Sea, we utilized $^{87}Sr/^{86}Sr$, $^{143}Nd/^{144}Nd$, Ba/Nb, and Rb/Zr ratios of volcanic products erupted during the past 800 k.y. In mafic volcanic rocks, the selected parameters have values characteristic of specific domains of the mantle (e.g., asthenospheric versus lithospheric; deeper versus shallower) from which they derived; also, these parameters vary mostly as a result of processes occurring in the mantle source of the magmas. In particular $^{87}Sr/^{86}Sr$ is very low, and $^{143}Nd/^{144}Nd$ is very high in magmas derived from shallow asthenospheric mantle, whereas they are higher and lower, respectively, in magmas derived from both deep asthenospheric and lithospheric mantle. Ratios of incompatible trace elements with different affinity for fluid phases, such as Ba/Nb and Rb/Zr ratios (both fluid mobile/fluid immobile element ratios) are higher in magmas derived from mantle sources in which the original mantle geochemistry has been modified (i.e., enriched) by subduction slab-derived fluids/melts carrying those elements, with respect to magmas derived from unmodified mantle. However, it is important to point out that these concepts are applicable only to mafic volcanic rocks, whereas in more differentiated volcanic rocks, the values of the selected parameters can change as the result of fractional crystallization and open-system evolution processes of magmas.

The data, compiled from the available literature, are plotted along a section (Fig. 5) that incorporates from SW to NE: Pantelleria, Ustica, Prometeo, Aeolian Islands (divided in three groups: Alicudi; Filicudi, Salina, Vulcano, Lipari, Panarea; Stromboli), Procida, Ischia, Campi Flegrei, Somma-Vesuvius, and Vulture. We also projected on the profile data

concerning Etna and the Tyrrhenian Sea mid-ocean-ridge basalt (MORB; Vavilov Basin, active between 4 and 3 Ma). To take into account the effects of fractionation, we filtered the chemical data to include rocks with MgO > 5 wt%, even though the scarcity of primitive compositions for some volcanoes is a serious limitation in the investigation of the selected geochemical and isotopic parameters in a larger range of rocks. For each volcano, we reported the lowest measured Sr-isotopic ratio and the highest measured Nd-isotopic ratio. For Tyrrhenian Sea MORB only, we utilized average values, since the few available $^{87}Sr/^{86}Sr$ and $^{143}Nd/^{144}Nd$ data are quite variable, especially $^{87}Sr/^{86}Sr$, which is at variance to what would be expected for this kind of rock, which are generally very homogeneous. Moreover, we report the average Ba/Nb and Rb/Zr ratios, to minimize effects of fractionation and contamination. The latter element/element ratios were chosen because arc magmas are characterized by high large ion lithophile elements/high field strength elements (LILE/HFSE) ratios, distinct from the trace-element distribution of anorogenic magmas. There is consensus that this enrichment is a consequence of fluid/melt-controlled partitioning of LILE relative to HFSE from the slab to the mantle wedge. The geochemical data are presented with the corresponding tomographic section, showing the along-strike prospective of the narrow Calabrian slab. The Aeolian arc and the Neapolitan volcanoes are characterized by products with higher Ba/Nb and Rb/Zr ratios, with respect to the Pantelleria, Ustica, Prometeo, Etna, and Tyrrhenian Sea basalts, which are considered to be the most representative of the African asthenospheric mantle (D'Antonio et al., 1996; Civetta et al., 1998). However, Etna is characterized by a slightly higher Rb/Zr ratio, suggesting a weak contribution from subduction-related components, as already suggested on the basis of other geochemical data (Beccaluva et al., 1982; Schiano et al., 2001; Tonarini et al., 2001). Vulture has Ba/Nb and Rb/Zr ratios comparable to those of the least LILE-enriched Aeolian arc products (AE1), and is thus intermediate between Pantelleria, Ustica, Prometeo, Etna, Tyrrhenian Sea basalts, and the Neapolitan volcanoes. These features have been used to infer a role for subduction-related components in the Vulture magma genesis that is more significant than for Etna (Beccaluva et al., 2002). The Sr-isotope ratio progressively increases from Pantelleria to the Neapolitan volcanoes, with a low value in the Tyrrhenian Sea basalts, and the highest values at Campi Flegrei and Somma-Vesuvius. The Vulture rocks display an isotopic composition less radiogenic than the Neapolitan volcanoes located inland, but comparable to the products of Ischia and Procida Islands. The Nd-isotope ratio displays a relationship similar to that of Sr but with a reversed trend, strongly suggesting that the overall Sr-Nd isotope variations are a result of mantle processes.

The patterns of the selected geochemical and isotopic tracers show rather distinct features that can be linked to the distribution of velocity anomalies in the southern Tyrrhenian mantle. The low Sr-isotope ratio in the Sicily Channel region is located on top of a low-velocity anomaly, whereas the Aeolian arc high Sr-isotope ratio is located on top of a high-velocity anomaly, the Calabrian slab. The high Sr-isotope ratio of Neapolitan volcanoes instead is located on top of the low-velocity anomaly located below the southern Apennines. This apparently contradictory feature will be discussed later.

MANTLE CIRCULATION AROUND A SLAB: LABORATORY EXPERIMENTS

With the aim of providing quantitative insights on mantle circulation in subduction zones, we performed 3-D laboratory experiments using models (Fig. 7A; Funiciello et al., 2004a). Our models, properly scaled to reflect the force balance in nature (Fig. 7B), have the advantage of realizing a self-consistent subduction in which the flow induced in the mantle by the slab is created and acts answering to the dynamics of the subduction process. Models have been built upon our previous efforts (Funiciello et al., 2003, 2004a; Bellahsen et al., 2005) by adding an apparatus able to quantitatively estimate the velocity field and mantle flow pattern using the Feature Tracking (FT) image analysis technique (Fig. 7A; Miozzi, 2004; Moroni and Cenedese, 2005).

Our results confirm the presence of a typical sequence of phases in the kinematic evolution of the subduction process as already described in Funiciello et al. (2003, 2004a). A steady-state regime, during which trench velocity and slab dip maintain constant values, is reached only after the slab–660 km discontinuity interaction. As additional outcome, we highlight the strong episodicity also in the toroidal mantle circulation.

The toroidal component of mantle circulation acts in the *x*-*y* plane from the beginning of the process (Fig. 8A) and is generated by the lateral slab migration. As a result, two symmetric toroidal return-flow cells form centered close to the plate edges (Fig. 8B). Each of the two cells has fixed dimensions linearly dependent on trench width (Funiciello et al., 2004a, 2004b) and follows the oceanward trench migration during the entire evolution of the process (Fig. 8A). The velocity field increases with time, consistent with trench velocity reaching its maximum before the slab interacts with the bottom of the box (Fig. 8A) and reaching a steady-state value only after slowdown caused by the slab–upper/lower mantle discontinuity interaction (Figs. 8A and 8B).

Velocity peak at each time is recorded in the region in front of the trench (Fig. 8A) and is assumed to be the value of v_t (expressing mantle velocity in terms of percentage of trench velocity allows an easier comparison between experimental results and natural cases). The lateral component of flow reaches its maximum velocity ~300–400 km away from the slab edge (Fig. 8A).

DISCUSSION: HISTORY OF SLAB DEFORMATION AND MANTLE CIRCULATION

The reconstruction and the data set presented here have several implications:

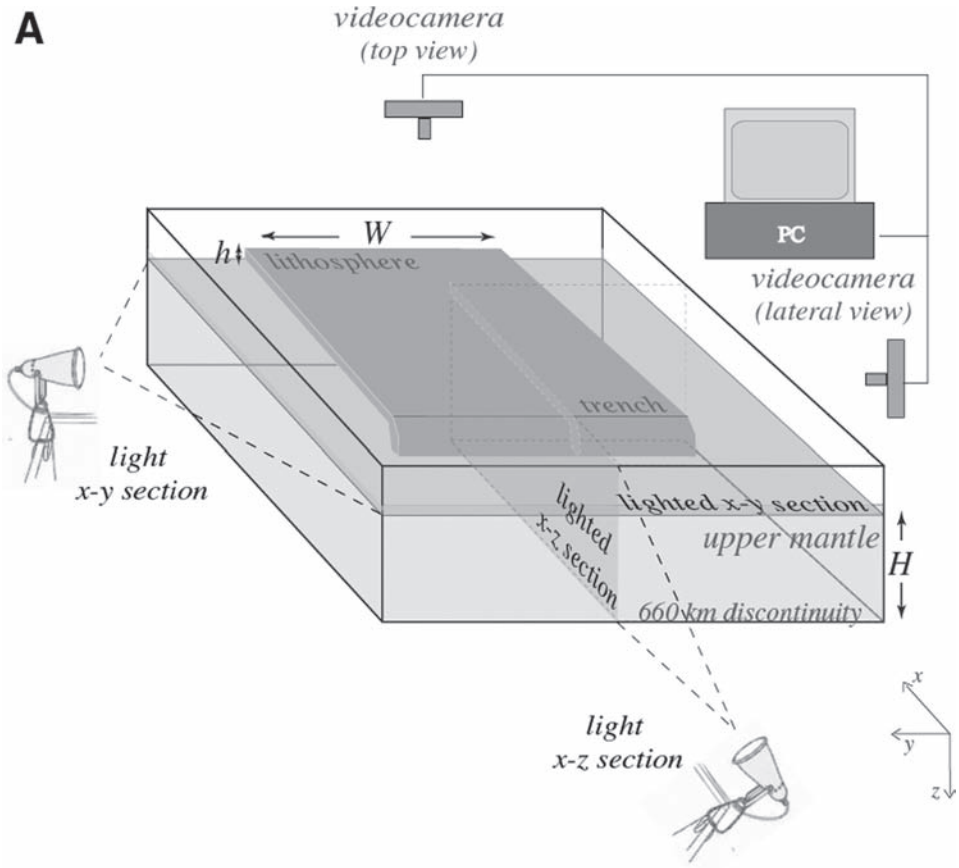

B

	PARAMETER		NATURE	MODEL
g	Gravitational acceleration	$m \times s^{-2}$	9.8	9.8
	Thickness			
h_l	Oceanic lithosphere	m	100000	0.016
H	Upper mantle		660000	0.11
	Scale factor for length		$L_{model}/L_{nature}=1.6\times 10^{-7}$	
	Density			
ρ_l	Oceanic lithosphere	$kg \times m^{-3}$	3300	1480
ρ_{um}	Upper mantle		3220	1415
	Density contrast (ρ_l-ρ_{um})		*80*	*65*
	Density ratio (ρ_l/ρ_{um})		*1.02*	*1.05*
	Viscosity			
η_l	Oceanic lithosphere	$Pa \times s$	10^{24}	$3.6\cdot10^{5}$ (± 5%)
η_{um}	Upper mantle		10^{20}	30 (± 20%)
	Viscosity ratio (η_l/η_{um})		10^{4}	$\sim 10^{4}$
t	**Characteristic time** $(t_{nature}/t_{model} = (\Delta\rho gh)_{lith\ model}/(\Delta\rho gh)_{lith\ nature} \cdot \eta_{l\ nature}/\eta_{l\ model})$	s	$3.1\cdot10^{13}$ (1 Myr)	~ 60 (~ 1 minute)

Figure 7. (A) Experimental set-up. The lithosphere is simulated with a silicone plate. The mantle is simulated with glucose syrup seeded with neutrally buoyant highly reflecting air microbubbles. The upper/lower mantle discontinuity is simulated by the bottom of the box, assuming that, for the limited time scale of the subduction process (<100 m.y.), it cannot directly penetrate into the 660 km discontinuity (Davies, 1995; Guillou-Frottier et al., 1995; Christensen, 1996; Funiciello et al., 2003). The subduction is started by manually bending the leading edge of the plate into the glucose syrup. Afterward, the subduction evolves in a dynamically self-consistent way. Experiments are monitored over their entire duration by two black-and-white progressive scan cameras in the lateral and top view. Trench retreat, dip of the slab, and mantle circulation patterns are systematically measured. In particular, analysis of toroidal mantle circulation is performed in the *x-y* plane just below the plate lighted by a neon light sheet of ~5 mm. With the aim to obtain a good resolution, after testing to make sure that the analyzed flow is symmetrical along the plate centerline, we investigated just half of the model (gray part). Postprocessing the recorded images with the Feature Tracking technique makes it possible to obtain a Lagrangian description of the velocity field that provides sparse velocity vectors with application points coincident with the bright reflecting microbubbles. (B) Scaling of parameters in nature and in laboratory. In particular, 1 cm and 1 min in the experiment corresponds to 60 km and 1 m.y. in nature, respectively.

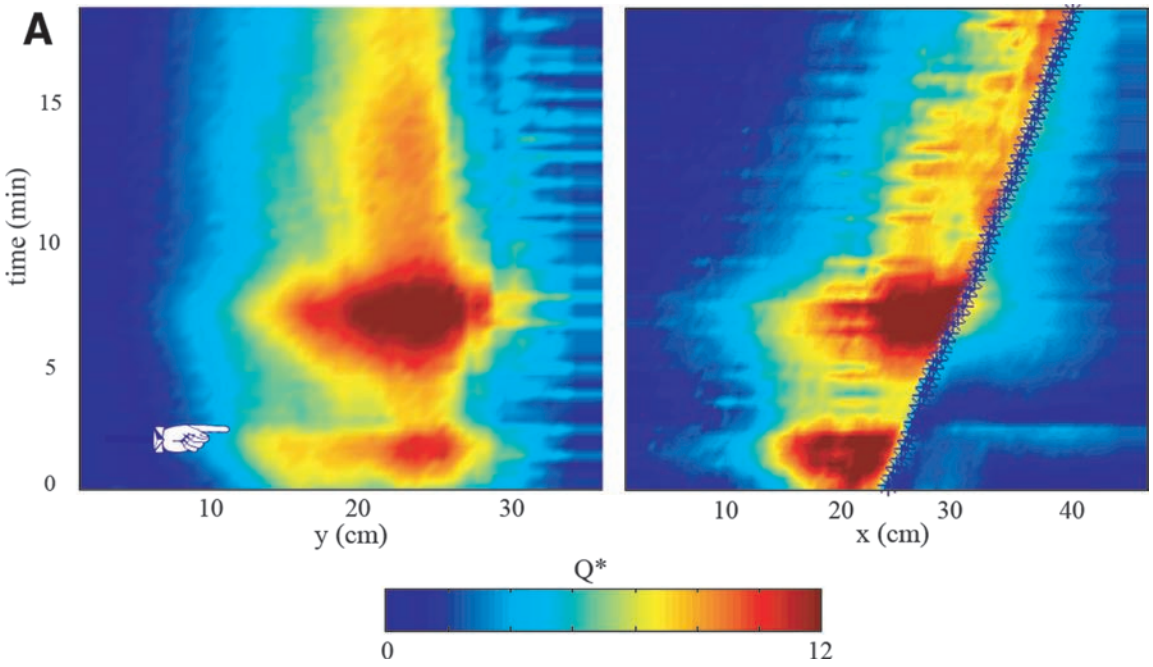

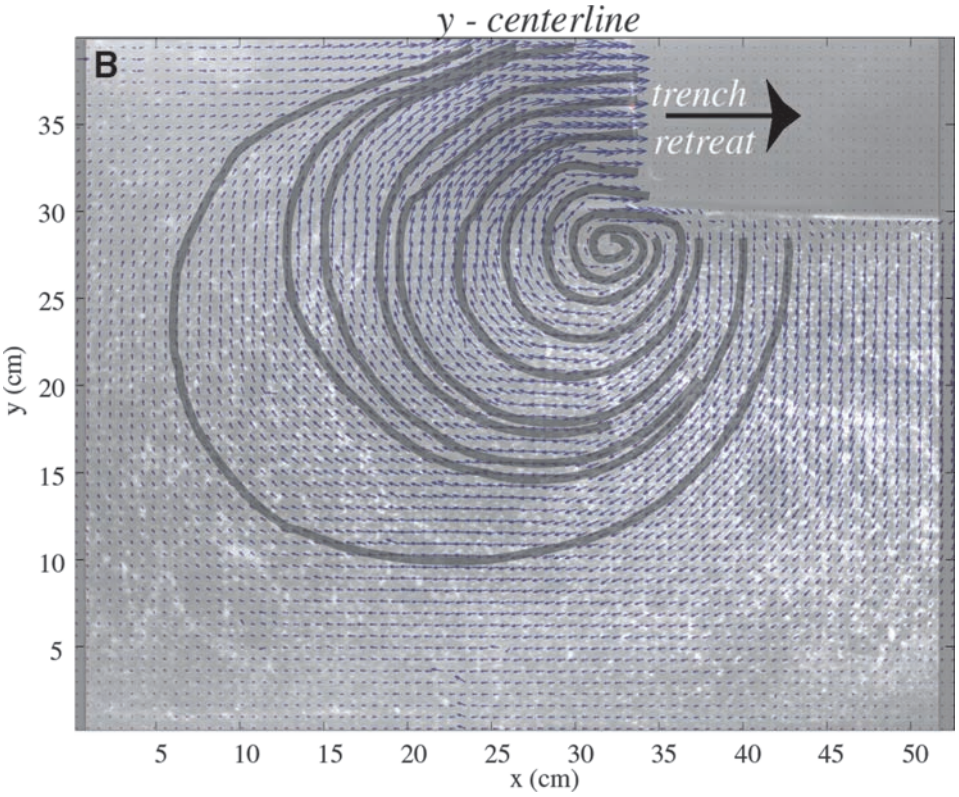

Figure 8. (A) Time-evolution of linear flux for both x and y component of mantle circulation. For coordinate system and scaling parameters, refer to Figures 7A and 7B, respectively. In order to visualize the entire evolution of the experiment, we introduced the time dependent linear absolute flux for both x and y components of the mantle velocity field. Flux components are $Q_x = \int |v_y dx|$ and $Q_y = \int |v_x dy|$. Q_x (Q_y) is computed by integrating the absolute value of v_y (v_x) along the x (y) direction. Hence, it depends on y (x) and time. Both components are normalized for a reference flux that was obtained by multiplying the characteristic trench velocity of the experiment by the plate thickness. To help the interpretation, we marked on the left panel the time of occurrence of the slab–660 km discontinuity interaction, when the mantle circulation temporarily slows down. The position of the trench motion at each time is indicated by asterisks on the right panel. This panel allows us to summarize the evolution of toroidal flow during the entire evolution of the experiment, highlighting its strong intermittent behavior. Q_x and Q_y show two peaks just before and after the slab–660 km discontinuity interaction. Steady-state regimes were established afterward, with flux constant through time. (B) Velocity field and streamlines of toroidal mantle circulation during the steady-state phase as obtained from the Feature Tracking analysis. The reference velocity shown at the top-left corner is 0.01 cm/s. Streamlines of mantle flow have limited interference with lateral box boundaries during the entire evolution of the experiment, confirming the laterally unconstrained character of our experimental setting (see Funiciello et al., 2004a, for details).

Episodic Backarc Extension

The opening of the Tyrrhenian Sea has been episodic (Kastens et al., 1988; Sartori et al., 1989; Faccenna et al., 1997, 2001b) (Fig. 9). Three key steps can be defined: the onset of extension (around 10 Ma) and the two different spreading events of the oceanic Tyrrhenian basins (Vavilov, 4–3 Ma; Marsili, 2–1 Ma) (Patacca et al., 1990; Nicolosi et al., 2006). These episodes match with the pulses of eastward space-time migration of the western edge of the flexural domain in the southern Tyrrhenian compressional thrust front region. The agreement between the two different sets of data pleads in favor of a common origin. In particular, combining this information with volcanological data and tomographic images, we suggest that the three pulses of deformation can be related to the formation and progressive enlargement of slab windows, both in the southern Tyrrhenian Sea and in the southern Apennines. One can argue that the age matching between the data is not robust, considering the short interval of time (10 m.y.) and the data uncertainties. There are, however, two geometrical considerations in support of this model. First, the (NNE-SSW) length of the backarc basins decreases, from the Sardinia Basin (around 350 km long) to the Vavilov (130 km) and the Marsili (70 km). This implies that the active retreating portion of the slab has been drastically reduced in time. Second, the locus of extension shifted gradually toward the east, but it always has been located north of the western tip of the active portion of the slab, as deduced by the age of flexural deposits (Casero, 2005). Therefore, it is reasonable to conclude that the backarc extension process is controlled by the geometry of the deforming subducting lithosphere. In other words, it is possible to infer that the lateral tear and separation of the Ionian slab from the contiguous buoyant continental domains permit its retrograde motion and, in turn, produce backarc extension. The episodic pulses of retreat are also in agreement with experimental findings, which show episodes of vigorous toroidal motion also after the interaction between the slab and the 660 km discontinuity (Fig. 8A). This model can be tested by kinematic information: experimental findings, in fact, show that a narrower slab retreats faster because subslab mantle material can easily turn around it (Funiciello et al., 2004a, 2004b; Bellahsen et al., 2005). In this model, we should then expect a quite rapid emplacement of the Marsili oceanic basin. For this reason, it is important to acquire new data on the age of the oceanic crust in the Vavilov and Marsili Basins.

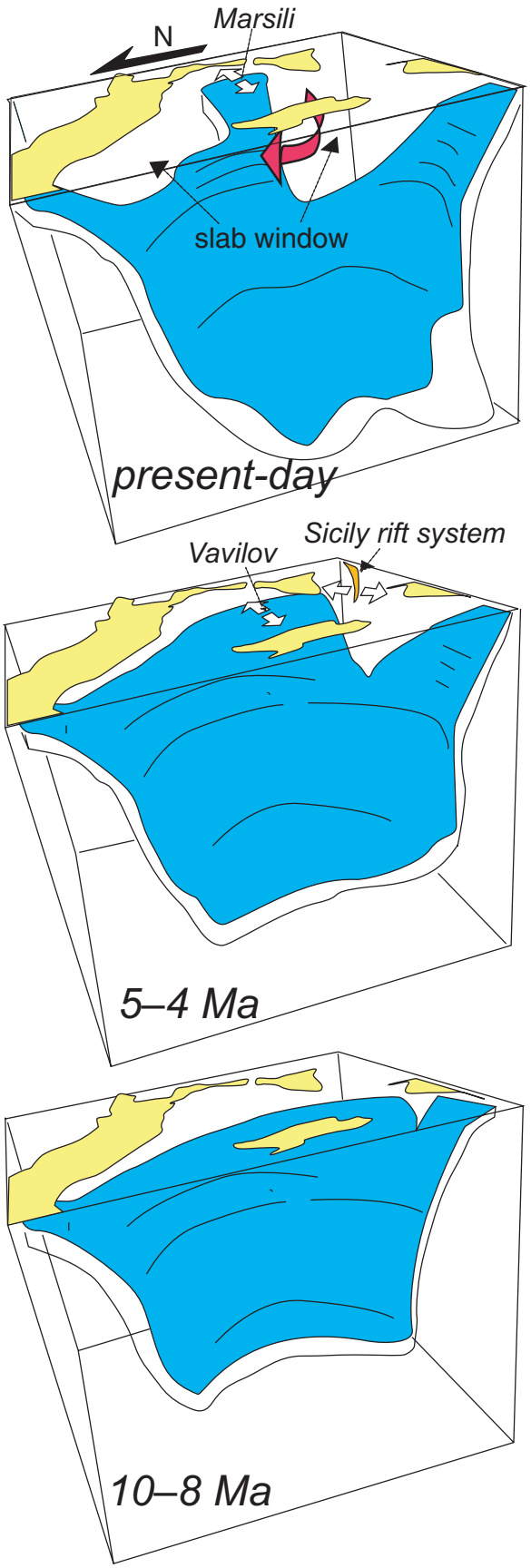

Figure 9. 3-D schematic tectonic reconstruction of the history of the central Mediterranean. Three key steps are shown: 10–8 Ma, 5–4 Ma, and today. In each panel, the geometry of the slab, the locus of backarc extension (white arrows), and the approximate mantle flow trajectories (gray arrow) are shown. In particular, the present-day distribution of the slab is derived from the tomographic image shown in Figure 4B.

Mantle-Flow Trajectories

Through the newly formed tectonic windows, the hotter subslab materials enter inside the backarc domain (Fig. 9).

In the southern Tyrrhenian region, the amount of mantle material flowing inside the backarc region has been large enough to change the composition of the erupted magmas from predominantly calc-alkaline to alkaline. This model can explain the position of Nefza and Mogods, and Ustica or Prometeo, which are all located in sites of previous calc-alkaline magmatism (i.e., Anchise). The volcanoes in the backarc zone that show alkaline anorogenic fingerprints are placed just north of the southern Tyrrhenian slab window. This implies that the flow was (and is) not strong enough to drastically modify the signature of the magmas feeding arc volcanoes (for example Aeolian arc or Anchise, located on top of the slab). Therefore, the pulses of alkali magmatism recently recorded in Sardinia or further north in Provençe require other explanations (Savelli, 2002). SKS splitting pattern in Sicily has been interpreted as related to lateral return flow turning around the western slab edge (Fig. 6 of Civello and Margheriti, 2004). The geochemical signatures agree with this model (Trua et al., 2003), indicating the way backarc mantle is contaminated by inflow of subslab (African) mantle material. Experimental test shown here, indeed, match the orientation of the splitting anisotropy, justifying the orientation of the N-S trend in western Sicily, but further tests are necessary to provide a quantitative comparison.

The Neapolitan volcanic district is located on top of the southern Apennine slab. Some tomographic models (see previous discussion) indicate the presence of a window (Figs. 1A and 3). If this is the case, its formation should have occurred after the cessation of the main thrusting phase, that is, around 700 ka (Patacca et al., 1990). However, its geochemical and petrological features, i.e., high radiogenic Sr and unradiogenic Nd contents and high LILE/HFSE ratios, suggest that the mantle beneath the Neapolitan region is still contaminated by subducted material (Figs. 2 and 5). This implies that either the slab window is not present or that the return flow was not efficient enough to produce a significant change of the mantle source; this is in agreement with SKS splitting pattern that preserves the regional trend NW-SE of the Apenninic chain (Fig. 6). Such an effect is possibly related to the time scale of the process. Comparing the scenario of the southern Apennines with the one of the southern Tyrrhenian domain, it can be deduced that to reorganize the mantle flow field to be seismologically and geochemically detected, a longer time is necessary (in the order of few million of years), with a flow rate of a few cm/yr (central Mediterranean average subduction velocity). In this frame, the Mt. Vulture volcano occupies a key position, as it is located east of the Neapolitan district, in a more external position. Mt. Vulture, indeed, shows an intermediate isotopic and geochemical composition of the two contrasting magmatic suites (Beccaluva et al., 2002). A possible way to interpret this feature is to imagine that the return flow below the Apennines is at an initial stage, only recognizable at Mt. Vulture, and it has yet to appear at the Neapolitan volcanoes. Geochemical and isotopical analysis of the oldest products would be important to define the existence of a possible trend toward anorogenic affinity also within the Neapolitan district.

Slab Disruption

Geological, volcanological data, and tomographic images indicate the presence of slab windows around the Calabrian slab, both in the southern Tyrrhenian Sea and, most probably, also below in the southern Apennines (Figs. 4B and 9). Several tectonic models have suggested the presence of a slab window around the Calabrian subduction zone (Lonergan and White, 1997; Carminati et al., 1998; Gvirtzman and Nur, 1999; Wortel and Spakman, 2000). However, it is still debated about how and why this slab deformed. Two possible reasons can be invoked explaining why the Calabrian slab broken from the rest of the African slab. First, the Ionian oceanic strip, once separated from the more buoyant African continental lithosphere, was able to sustain its retrograde motion. Second, the rupture of the subducted lithosphere also enhanced the dissipation of the mantle overpressure created below the slab during its retrograde motion (Garfunkel et al., 1986; Faccenna et al., 2001b; Funiciello et al., 2003). Once the slab interacted with the 660 km discontinuity, the overpressure in the subslab mantle material was high enough to slow down the slab retrograde motion (Garfunkel et al., 1986; Faccenna et al., 2001b) and to induce the lateral slab deformation and its eventual break (Funiciello et al., 2003). From this moment on, the retreat of the slab was achieved by the lateral escape of subslab mantle material from the sides of the deformed slab.

The Calabrian slab provides a unique occasion to describe properly its long-term evolution, including the timing and the magnitude of its internal deformation. The locus of the initial deformation is somehow problematic. Most commonly, in fact, the opening of slab windows requires the entrance at a trench of buoyant lithospheric discontinuities, such as transform faults or aseismic ridges. This occurred in California during the Eocene, and in western Antarctica (Thorkelson, 1996) or in the Kamchatka-Aleutian subduction zone, where the slab window is placed in correspondence of the Meiji-Emperor-Hawaiian hotspot chain (Davaille and Lees, 2004). The lateral rupture of the Calabrian arc in the southern Tyrrhenian Sea, however, did not correspond with the pre-existing Mesozoic margin of the Ionian ocean but was located inside the Pelagian plateau (Figs. 3 and 9), which does not present traces of large pre-existing tectonic structures. We note, however, that prior to the opening of the Tyrrhenian Sea, the slab should have attained a rather sharp curvature just south of Sardinia to accommodate the opening of the Liguro-Provençal and Algerian Basins. If this was the case, this area could be the more suitable to localize deformation. Apart from its initiation, the mechanism of window opening also remains enigmatic. If the opening was due to the migration of the active portion of the slab to the E-SE relative to Tunisia, one should expect a large extensional/transtensional rift zone lacer-

ating the subducting plate and its foreland. The opening of the Sicily Channel rift zone could have developed in response of this mechanism. The Sicily Channel rift system is a narrow rift system and shows a significant crustal attenuation (Suhadolc and Panza, 1989) with Moho rising up to 20 km depth with respect to its shoulder, which stands at 30 km depth. A gross estimation of the amount of extension leads to ~50 km. This value is far too low to explain the 400-km-wide window in the subducting slab. Mechanical and thermal erosion could have also participated in eroding the slab, the latter especially considering the low rate of subduction (1–2 cm/yr). Davaille and Lees (2004) analyzed this possibility for the Kamchatka-Aleutian junction and showed that thermal erosion at the slab edge cannot be an efficient mechanism to enhance the slab erosion. Mechanical erosion, already explored for the Kamchatka-Aleutian by Levin et al. (2002), supposes that the edge of the slab can be progressively eroded by the toroidal component of the return flow. In the Tyrrhenian subduction, the slab disruption mechanism should have removed a total of ~3.5 million km^3 of slab in two distinct episodes involving an area of ~43,000 km^2. Each episode of slab loss was likely accompanied by volcanic episodes with an imprinting of subslab mantle material, indicating massive invasion of hot material in the subduction wedge replacing the slab. The present-day positions of the slab portions are difficult to identify because in the central Mediterranean, a huge mass of lithospheric material is presently stagnating on the 660 km discontinuity (Fig. 4B).

Below the southern Apennines, the mechanism could have been different, and the vertical detachment of the oceanic portion of the slab from the buoyant continental portion could have enhanced the formation of a slab window. However, the southern Tyrrhenian Sea and the southern Apennines slab window should have formed contemporaneously, producing a dramatic change in the tectonic regime of the entire region. Rapid and intermittent loss of a huge mass of slab material during the last million years could have caused dramatic reorganization of mantle convection, reducing the lateral length of the Calabrian slab to a small finger-like structure plunging down into the mantle. If this is the case, we can use Calabria as an outstanding example to investigate the way subduction ends. The ideas that a slab can easily be consumed at its edge and that subduction can end rapidly in few million of years support the possibility of rapid global reorganization of mantle convection (King et al., 2002).

CONCLUSION

We have described the evolution of the Calabrian subduction zone by combining plate tectonic history, geological, geochemical and seismological data, and laboratory modeling. The key to this analysis is that the narrow and rapidly retreating Calabrian slab results from the lateral disruption of the western Mediterranean subduction zone produced by the formation of two large windows, in the southern Tyrrhenian Sea and in the southern Apennines. We analyzed and defined the timing and extent of these slab breaks using both geological and geochemical data and tomographic images. We speculate that the Calabrian slab has been progressively eroded by means of mechanical and thermal processes.

We speculate that windows at lateral slab edges have caused an episodic reorganization of mantle convection, permitting inflow of anomalous subslab mantle material into the mantle wedge and causing a complicated pattern of magmatism in the Tyrrhenian region, resulting in the pattern of close association of alkaline and calc-alkaline products. The episodicity can be read also in the discrete opening of the inner Tyrrhenian backarc basins, which occurred in three phases of deformation (10–8 Ma, 5–6 Ma, and 1–0.8 Ma).

The model presented here gives insights into the long-term evolution of the Calabrian subduction. The model suggests that the rapid and intermittent loss of a huge mass of material at the slab edges progressively reduces the lateral length of the Calabrian slab and enhances the progressive increase of roll-back velocity, which is in agreement with experimental results of Bellahsen et al. (2005). In the final phase, the slab is too tiny to subduct actively, and so it passively steepens under its own weight, enhancing the end of the subduction process.

ACKNOWLEDGMENTS

The authors thank the editors L. Beccaluva, G. Bianchini, and M. Wilson. The work benefited from the scientific discussion by D. Giardini, T. Becker, A. Cenedese, F. Speranza, and the critical reviews by E. Carminati and A. Hasegawa. Thanks are due to H.A. Bui for technical assistance in laboratory. Laboratory experiments were performed in the Laboratory of Tectonics (University of Roma Tre). We are grateful to *Syral srl* for providing us the glucose syrup used in our experimental models.

REFERENCES CITED

Alvarez, W., Cocozza, T., and Wezel, F.C., 1974, Fragmentation of the Alpine orogenic belt by microplate dispersal: Nature, v. 248, p. 309–314, doi: 10.1038/248309a0.

Anderson, H., and Jackson, J., 1987, The deep seismicity of the Tyrrhenian Sea: Geophysical Journal Royal Astronomy Society, v. 91, p. 613–637.

Argnani, A., 1990, The strait of Sicily rift zone: Foreland deformation related to the evolution of a back-arc basin: Journal of Geodynamics, v. 12, p. 311–331, doi: 10.1016/0264-3707(90)90028-S.

Argnani, A., Cornini, S., Torelli, L., and Zitellini, N., 1987, Diachronous foredeep-system in the Neogene-Quaternary of the Strait of Sicily: Memorie Società Geologica Italiana, v. 38, p. 407–417.

Beccaluva, L., Rossi, P.L., and Serri, G., 1982, Neogene to recent volcanism of the southern Tyrrhenian–Sicilian area: Implications for the geodynamic evolution of the Calabrian arc: Earth Evolution Sciences, v. 3, p. 221–238.

Beccaluva, L., Brotzu, P., Macciotta, G., Morbidelli, L., Serri, G., and Traversa, G., 1989, Cenozoic tectono-magmatic evolution and inferred mantle sources in the Sardo-Tyrrhenian area, *in* Boriani, A., Bonafede, M., Piccardo, G.B., and Vai, G.B., eds., The Lithosphere in Italy: Advances in science research: Roma, Accademia Nazionale dei Lincei, p. 229–248.

Beccaluva, L., Di Girolamo, P., and Serri, G., 1991, Petrogenesis and tectonic setting of the Roman volcanic province, Italy: Lithos, v. 26, p. 191–221, doi: 10.1016/0024-4937(91)90029-K.

Beccaluva, L., Coltorti, M., Galassi, R., Macciotta, G., and Siena, F., 1994, The Cenozoic calcalkaline magmatism of the western Mediterranean and its geodynamic significance: Bollettino Geofisica Teorica Applicata, v. 36, p. 293–308.

Beccaluva, L., Siena, F., Coltorti, M., Di Grande, A., Lo Giudice, A., Macciotta, G., Tassinari, R., and Vaccaro, C., 1998, Nephelinitic to tholeiitic magma generation in a transtensional tectonic setting: An integrated model for the Iblean volcanism, Sicily: Journal of Petrology, v. 39, p. 1547–1576, doi: 10.1093/petrology/39.9.1547.

Beccaluva, L., Coltorti, M., Di Girolamo, P., Melluso, L., Milani, L., Morra, L., and Siena, F., 2002, Petrogenesis and evolution of Mt. Vulture alkaline volcanism (southern Italy): Mineralogical Petrology, v. 74, p. 277–297, doi: 10.1007/s007100200007.

Beccaluva, L., Bianchini, G., Coltorti, M., Siena, F., and Verde, M., 2005a, Cenozoic tectono-magmatic evolution of the central-western Mediterranean: Migration of an arc-interarc basin system and variations in the mode of subduction, *in* Finetti, I. ed., Crop Project—Deep Seismic Exploration of the central Mediterranean and Italy: Elsevier special volume, p. 623–640.

Beccaluva, L., Bianchini, G., Bonadiman, C., Coltorti, M., Macciotta, G., Siena, F., and Vaccaro, C., 2005b, Within-plate Cenozoic volcanism and lithospheric mantle evolution in the western-central Mediterranean area, *in* Finetti, I. ed., Crop Project—Deep Seismic Exploration of the central Mediterranean and Italy: Elsevier special volume, p. 641–664.

Bellahsen, N., Faccenna, C., and Funiciello, F., 2005, Dynamics of subduction and plate motion in laboratory experiments: Insights into the "plate tectonics" behavior of the Earth: Journal of Geophysical Research, v. 110, no. B01401, doi: 10.1029/2004JB002999.

Bertotti, G., Picotti, V., Chilovi, C., Fantoni, R., Merlini, S., and Mosconi, A., 2001, Neogene to Quaternary sedimentary basins in the south Adriatic (central Mediterranean): Foredeeps and lithospheric buckling: Tectonics, v. 20, p. 771–787, doi: 10.1029/2001TC900012.

Burrus, J., 1984, Contribution to a geodynamic synthesis of the Provencal Basin (north-western Mediterranean): Marine Geology, v. 55, p. 247–269, doi: 10.1016/0025-3227(84)90071-9.

Carminati, E., Wortel, R., Spakman, W., and Sabadini, R., 1998, The role of slab-detachment processes in the opening of the western-central Mediterranean basins: Some geological and geophysical evidence: Earth and Planetary Science Letters, v. 160, p. 651–665, doi: 10.1016/S0012-821X(98)00118-6.

Carminati, E., Negredo, A.M., Valera, J.L., and Doglioni, C., 2005, Subduction-related intermediate-depth and deep seismicity in Italy: Insights from thermal and rheological modelling: Physics of the Earth and Planetary Interiors, v. 149, p. 65–79, doi: 10.1016/j.pepi.2004.04.006.

Casero, P., 2005, Structural setting of petroleum exploration plays in Italy, *in* Crescenti, U. et al., eds., Geology of Italy: Special Volume, Bollettino Società Geologica Italiana, p. 189–200.

Casero, P., and Roure, F., 1994, Neogene deformations at the Sicilian–North African plate boundary, *in* Roure, F., ed., PeriTethyan Platforms: Paris, Ed. Technip., P. 27–45.

Chamot-Rooke, N., Gaulier, J.M., and Jestin, F., 1999, Constraints on Moho depth and crustal thickness in the Liguro-Provençal Basin from a 3D gravity inversion: Geodynamic implications, *in* Durand, B., Mascle, A., Jolivet, L., Horvàth, F., and Séranne, M., eds., The Mediterranean Basins: Tertiary Extension within the Alpine Orogen: Geological Society of London Special Publication 156, p. 37–61.

Cherchi, A., and Montandert, L., 1982, Oligo-Miocene rift of Sardinia and the early history of the western Mediterranean Basin: Nature, v. 298, p. 736–739, doi: 10.1038/298736a0.

Christensen, U.R., 1996, The influence of trench migration on slab penetration into the lower mantle: Earth and Planetary Science Letters, v. 140, p. 27–39.

Cinque, A., Civetta, L., Orsi, G., and Peccerillo, A., 1988, Geology and geochemistry of the island of Ustica (southern Tyrrhenian Sea): Rendiconti della Società Italiana di Mineralogia e Petrologia, v. 43, p. 987–1002.

Civello, S., and Margheriti, L., 2004, Toroidal mantle flow around the Calabrian slab (Italy) from SKS splitting: Geophysical Research Letters, v. 31, p. L10601, doi: 10.1029/2004GL019607.

Civetta, L., D'Antonio, M., Orsi, G., and Tilton, G.R., 1998, The geochemistry of volcanic rocks from Pantelleria Island, Sicily Channel: Petrogenesis and characteristics of the mantle source region: Journal of Petrology, v. 39, p. 1453–1491, doi: 10.1093/petrology/39.8.1453.

Conder, J.A., Wiens, D.A., and Morris, J., 2002, On the decompression melting structure at volcanic arcs and back-arc spreading centers: Geophysical Research Letters, v. 29, no. 15, p. 1–14, doi: 10.1029/2002GL015390.

D'Antonio, M., Tilton, G.R., and Civetta, L., 1996, Petrogenesis of Italian alkaline lavas deduced from Pb-Sr-Nd relationships, *in* Basu, A., and Hart, S.R., eds., Earth Processes: Reading the Isotopic Code: American Geophysical Union Geophysical Monograph 95, p. 253–267.

D'Antonio, M., Civetta, L., and Di Girolamo, P., 1999, Mantle source heterogeneity in the Campanian region (south Italy) as inferred from geochemical and isotopic features of mafic volcanic rocks with shoshonitic affinity: Mineralogy and Petrology, v. 67, p. 163–192, doi: 10.1007/BF01161520.

Davaille, A., and Lees, J.M., 2004, Thermal modeling of subducted plates: Tear and hotspot at the Kamchatka corner: Earth and Planetary Science Letters, v. 226, p. 293–304, doi: 10.1016/j.epsl.2004.07.024.

Davies, G.F., 1995, Penetration of plates and plumes through the mantle transition zone: Earth and Planetary Science Letters, v. 133, p. 507–516.

Davies, J.H., and Stevenson, D.J., 1992, Physical model of source region of subduction zone volcanics: Journal of Geophysical Research, v. 97, no. B2, p. 2037–2070.

De Astis, G., Peccerillo, A., Kempton, P.D., La Volpe, L., and Wu, T.W., 2000, Transition from calc-alkaline to potassium-rich magmatism in subduction environments: Geochemical and Sr, Nd, Pb isotopic constraints from the island of Vulcano (Aeolian arc): Contributions to Mineralogy and Petrology, v. 139, p. 684–703, doi: 10.1007/s004100000172.

De Gori, P., Cimini, G.P., Chiarabba, C., De Natale, G., Troise, C., and Deschamps, A., 2001, Teleseismic tomography of the Campanian volcanic area and surrounding Apenninic belt: Journal of Volcanology and Geothermal Research, v. 109, p. 55–75, doi: 10.1016/S0377-0273(00)00304-8.

Del Moro, A., Gioncada, A., Pinarelli, L., Sbrana, A., and Joron, J.L., 1998, Sr, Nd and Pb isotope evidence of open system evolution at Vulcano (Aeolian arc, Italy): Lithos, v. 43, p. 81–106, doi: 10.1016/S0024-4937(98)00008-5.

De Long, S.E., Hodges, F.N., and Arculus, R.J., 1975, Ultramafic and mafic inclusions, Kanaga Island, Alaska, and the occurrence of alkaline rocks in island arcs: Journal of Geology, v. 83, p. 721–736.

Deschamps, A., and Lallemand, S., 2003, Geodynamic setting of Izu-Bonin-Mariana boninites, *in* Larter, R.D., and Leat, P.T., eds., Intra-Oceanic Subduction Systems: Tectonic and Magmatic Processes: Geological Society of London Special Publication, p. 163–185.

Dewey, J.F., Helman, M.L., Turco, E., Hutton, D.H.W., and Knott, S.D., 1989, Kinematics of the western Mediterranean, *in* Coward, M.P., Dietrich, D., and Park, R.G., eds., Alpine Tectonics: Geological Society of London Special Publication 45, p. 265–283.

Di Girolamo, P., Nardi, G., Rolandi, G., and Stanzione, D., 1976, Occurrence of calc-alkaline two-pyroxene andesites from deep bore-holes in the Phlegraean Fields. I. Petrographic and petrochemical data: Rendiconti dell'Accademia di Scienze Fisiche e Matematiche in Napoli, v. 43, p. 45–73.

Doglioni, C., Merlini, S., and Cantarella, G., 1999, Foredeep geometries at the front of the Apennines in the Ionian Sea (central Mediterranean): Earth and Planetary Science Letters, v. 168, p. 243–254, doi: 10.1016/S0012-821X(99)00059-X.

Doglioni, C., Innocenti, F., and Mariotti, G., 2001, Why Mt. Etna?: Terra Nova, v. 13, p. 25–31.

Eberle, M.A., Grasset, O., and Sotin, C., 2002, A numerical study of the interaction between the mantle wedge, subducting slab and over-riding plate: Physics of the Earth and Planetary Interiors, v. 134, p. 191–202.

Ellam, R.M., Hawkesworth, C.J., Menzies, M.A., and Rogers, N.W., 1989, The volcanism of southern Italy: Role of subduction and the relationship between potassic and sodic alkaline magmatism: Journal of Geophysical Research, v. 94, p. 4589–4601.

Faccenna, C., Mattei, M., Funiciello, R., and Jolivet, L., 1997, Styles of back-arc extension in the central Mediterranean: Terra Nova, v. 9, p. 126–130.

Faccenna, C., Becker, T.W., Lucente, F.P., Jolivet, L., and Rossetti, F., 2001a, History of subduction and back-arc extension in the central Mediterranean: Geophysical Journal International, v. 145, no. 3, p. 809–820, doi: 10.1046/j.0956-540x.2001.01435.x.

Faccenna, C., Funiciello, F., Giardini, D., and Lucente, P., 2001b, Episodic back-arc extension during restricted mantle convection in the central Mediterranean: Earth and Planetary Science Letters, v. 187, no. 1–2, p. 105–116, doi: 10.1016/S0012-821X(01)00280-1.

Faccenna, C., Jolivet, L., Piromallo, C., and Morelli, A., 2003, Subduction and the depth of convection in the Mediterranean mantle: Journal of Geophysical Research, v. 108, no. B2, p. 2099, doi: 10.1029/2001JB001690.

Faccenna, C., Piromallo, C., Crespo-Blanc, A., Jolivet, L., and Rossetti, F., 2004, Lateral slab deformation and the origin of the western Mediterranean arcs: Tectonics, v. 23, no. TC1012, p. 1–21, doi: 10.1029/2002TC001488.

Fischer, K.M., Parmentier, E.M., Stine, A.R., and Wolf, E.R., 2000, Modeling anisotropy and plate-driven flow in the Tonga subduction zone back arc: Journal of Geophysical Research, v. 105, no. B7, p. 16,181–16,191, doi: 10.1029/1999JB900441.

Francalanci, L., Taylor, S.R., McCulloch, M.T., and Woodhead, J.D., 1993, Geochemical and isotopic variations in the calc-alkaline rocks of Aeolian arc, southern Tyrrhenian Sea, Italy: Constraints on magma genesis: Contributions to Mineralogy and Petrology, v. 113, p. 300–313, doi: 10.1007/BF00286923.

Funiciello, F., Faccenna, C., Giardini, D., and Regenauer-Lieb, K., 2003, Dynamics of retreating slabs (part 2): Insights from 3D laboratory experiments: Journal of Geophysical Research, v. 108, no. B4, p. 1–16, doi: 10.1029/2001JB000896.

Funiciello, F., Faccenna, C., and Giardini, D., 2004a, Role of lateral mantle flow in the evolution of subduction system: Insights from 3-D laboratory experiments: Geophysical Journal International, v. 157, p. 1393–1406, doi: 10.1111/j.1365-246X.2004.02313.x.

Funiciello, F., Piromallo, C., Moroni, M., Faccenna, C., Becker, T.W., Bui, H.A., and Cenedese, A., 2004b, 3-D laboratory and numerical models of mantle flow in subduction zones: Eos (Transactions, American Geophysical Union), v. 85(47), Fall Meeting supplement, abstract T21B–0527.

Garfunkel, Z., Anderson, D.L., and Schubert, G., 1986, Mantle circulation and lateral migration of subducting slabs: Journal of Geophysical Research, v. 91, p. 7205–7223.

Gasperini, D., Blichert-Toft, J., Bosch, D., Del Moro, A., Macera, P., and Albarède, F., 2002, Upwelling of deep mantle material through a plate window: Evidence from the geochemistry of Italian basaltic volcanics: Journal of Geophysical Research, v. 107, no. 2367, doi: 10.1029/2001JB000418.

Giardini, D., and Velonà, M., 1991, The deep seismicity of the Tyrrhenian Sea: Terra Nova, v. 3, p. 57–64.

Gorini, C., Mauffret, A., Guennoc, P., and Le Marrec, A., 1994, Structure of the Gulf of Lions (northwestern Mediterranean Sea): A review, *in* Mascle, A., ed., Hydrocarbon and Petroleum Geology of France: London, European Association of Petroleum Geologists, p. 223–243.

Guillou-Frottier, L., Buttles, J., and Olson, P., 1995, Laboratory experiments on structure of subducted lithosphere: Earth and Planetary Science Letters, v. 133, p. 19–34.

Gvirtzman, Z., and Nur, A., 1999, The formation of Mt. Etna as the consequence of slab rollback: Nature, v. 401, p. 782–785, doi: 10.1038/44555.

Horvath, F., and Berckhermer, H., 1982, Mediterranean back-arc basin in Alpine Mediterranean geodynamics, *in* Berckhemer, H., and Hsu, K.J., eds., Alpine Mediterranean Geodynamics: Washington, D.C., American Geophysical Union, p. 145–175.

Jolivet, L., and Faccenna, C., 2000, Mediterranean extension and the Africa-Eurasia collision: Tectonics, v. 19, no. 6, p. 1095–1106, doi: 10.1029/2000TC900018.

Kastens, K.A., Mascle, J., and Party, O.L.S., 1988, ODP Leg 107 in the Tyrrhenian Sea: Insights into passive margin and backarc basin evolution: Geological Society of America Bulletin, v. 100, p. 1140–1156, doi: 10.1130/0016-7606(1988)100<1140:OLITTS>2.3.CO;2.

Kincaid, C., and Griffiths, R.W., 2003, Laboratory models of the thermal evolution of the mantle during rollback subduction: Nature, v. 425, p. 58–62, doi: 10.1038/nature01923.

King, S.D., Lowman, J.P., and Gable, C.W., 2002, Episodic tectonic plate reorganizations driven by mantle convection: Earth and Planetary Science Letters, v. 203, p. 83–91, doi: 10.1016/S0012-821X(02)00852-X.

Leat, P.T., Pearce, J.A., Barker, P.F., Millar, I.L., Barry, T.L., and Larter, R.D., 2004, Magma genesis and mantle flow at subducting slab edge: The South Sandwich arc-basin system: Earth and Planetary Science Letters, v. 227, p. 17–35, doi: 10.1016/j.epsl.2004.08.016.

Le Pichon, X., 1982, Land-locked ocean basin and continental collision in the eastern Mediterranean area as a case example: Mountain building processes: London, Academic Press, p. 201–213.

Levin, V., Shapiro, N., Park, J., and Ritzwoller, M., 2002, Seismic evidence for catastrophic slab loss beneath Kamchatka: Nature, v. 418, p. 763–767, doi: 10.1038/nature00973.

Lonergan, L., and White, N.J., 1997, The origin of the Betic Rif mountain chains: Tectonics, v. 16, p. 504–522, doi: 10.1029/96TC03937.

Lucente, F., Chiarabba, C., and Cimini, G., 1999, Tomographic constraints on the geodynamic evolution of the Italian region: Journal of Geophysical Research, v. 104, no. B9, p. 20,307–20,327, doi: 10.1029/1999JB900147.

Malinverno, A., and Ryan, W., 1986, Extension in the Tyrrhenian Sea and shortening in the Apennines as result of arc migration driven by sinking of the lithosphere: Tectonics, v. 5, p. 227–245.

Marani, M., and Trua, T., 2002, Thermal constriction and slab tearing at the origin of a super-inflated spreading ridge, Marsili volcano (Tyrrhenian Sea): Journal of Geophysical Research, v. 107, no. 2188, doi: 10.1029/2001JB000285.

Mattei, M., Cipollari, P., Cosentino, D., Argentieri, A., Rossetti, F., and Speranza, F., 2002, The Miocene tectonic evolution of the southern Tyrrhenian Sea: Stratigraphy, structural and paleomagnetic data from the on-shore Amantea Basin (Calabrian arc, Italy): Basin Research, v. 14, p. 147–168, doi: 10.1046/j.1365-2117.2002.00173.x.

Mattei, M., Petrocelli, V., Lacava, D., and Schiattarella, M., 2004, Geodynamic implications of Pleistocene ultrarapid vertical-axis rotations in the southern Apennines, Italy: Geology, v. 32, p. 789–792, doi: 10.1130/G20552.1.

Mauffret, A., Pascal, G., Maillard, A., and Gorini, C., 1995, Tectonics and deep structure of the north-western Mediterranean Basin: Marine and Petroleum Geology, v. 12, no. 6, p. 645–666, doi: 10.1016/0264-8172(95)98090-R.

Mauffret, A., Frizon de Lamotte, D., Lallemand, S., Gorini, C., and Maillard, A., 2004, E–W opening of the Algerian Basin (western Mediterranean): Terra Nova, v. 16, p. 257–264, doi: 10.1111/j.1365-3121.2004.00559.x.

Miozzi, M., 2004, Particle image velocimetry using Feature Tracking and Delauny Tessellation., *in* 12th International Symposium on Application of Laser Techniques to Fluid Mechanics: Lisbon.

Morelli, A., and Dziewonski, A.M., 1993, Body wave travel-times and a spherically symmetric P- and S-wave velocity model: Geophysical Journal International, v. 112, p. 178–194.

Moroni, M., and Cenedese, A., 2005, Comparison among Feature Tracking and more consolidated velocimetry image analysis techniques in a fully developed turbulent channel flow: Measurement Science & Technology, v. 16, p. 2307–2322, doi: 10.1088/0957-0233/16/11/02.

Muller, C., 2001, Upper mantle seismic anisotropy beneath Antarctica and Scotia Sea region: Geophysical Journal International, v. 147, p. 105–122, doi: 10.1046/j.1365-246X.2001.00517.x.

Nicolosi, I., Speranza, F., Chiappini, M., 2006, Ultrafast oceanic spreading of the Marsili Basin, southern Tyrrhenian Sea: Evidence from magnetic anomaly analysis: Geology, v. 34, p. 717–720, doi: 10.1130/G22555.1

Patacca, E., Sartori, R., and Scandone, P., 1990, Tyrrhenian Basin and Apenninic arcs: Kinematic relations since late Tortonian times: Memorie della Società Geologica Italiana, v. 45, p. 425–451.

Pearce, J.A., 1982, Trace element characteristics of lavas from destructive plate boundaries, *in* Thorpe, R.S., ed., Andesites: New York, Chichester, Wiley, p. 525–548.

Pearce, J.A., Leat, P.T., Bearker, P.F., and Millar, I.L., 2001, Geochemical tracing of Pacific to Atlantic upper-mantle flow through the Drake Passage: Nature, v. 410, p. 457–461, doi: 10.1038/35068542.

Peccerillo, A., 1999, Multiple mantle metasomatism in central-southern Italy: Geochemical effects, timing and geodynamic implications: Geology, v. 27, p. 315–318, doi: 10.1130/0091-7613(1999)027<0315:MMMICS>2.3.CO;2.

Peyton, V., Levin, V., Park, J., Brandon, M.T., Lees, J., Gordeev, E., and Ozerov, A., 2001, Mantle flow at a slab edge: Seismic anisotropy in the Kamchatka region: Geophysical Research Letters, v. 28, p. 379–382, doi: 10.1029/2000GL012200.

Piromallo, C., and Faccenna, C., 2004, How deep can we find the traces of Alpine subduction?: Geophysical Research Letters, v. 31, L06605, doi: 10.1029/2003GL019288.

Piromallo, C., and Morelli, A., 1997, Imaging the Mediterranean upper mantle by P-wave travel time tomography: Annales Geophysicae, v. 40, p. 963–979.

Piromallo, C., and Morelli, A., 2003, P-wave tomography of the top 1000 km under the Alpine-Mediterranean area: Journal of Geophysical Research, v. 108 (B2), no. 2065, doi: 10.1029/2002JB001757.

Roca, E., Sans, M., Cabrera, L., and Marzo, M., 1999, Oligocene to middle Miocene evolution of the central Catalan margin (northwestern Mediterranean): Tectonophysics, v. 315, p. 209–233, doi: 10.1016/S0040-1951(99)00289-9.

Russo, R.M., and Silver, P.G., 1994, Trench-parallel flow beneath the Nazca plate from seismic anisotropy: Science, v. 263, no. 5150, p. 1105–1111.

Sagnotti, L., 1992, Paleomagnetic evidence for a Pleistocene counterclockwise rotation of the Sant'Arcangelo Basin, southern Italy: Geophysical Research Letters, v. 19, p. 135–138.

Sartori, R., and Staff, O.L.S., 1989, Drillings of ODP Leg 107 in the Tyrrhenian Sea: Tentative basin evolution compared to deformations in the surrounding chains, *in* Boriani, A., Bonafede, M., Piccardo, G.B., and Vai, G.B., eds., The Lithosphere in Italy: Advances in Earth Science Research: Rome, Accademia Nazionale dei Lincei, p. 139–156.

Sartori, R., Carrara, G., Torelli, L., and Zitellini, N., 2001, Neogene evolution of the southwestern Tyrrhenian Sea (Sardinia Basin and western bathyal plain): Marine Geology, v. 175, p. 47–66, doi: 10.1016/S0025-3227(01)00116-5.

Savelli, C., 2002, Time-space distribution of magmatic activity in the western Mediterranean and peripheral orogens during the past 30 Ma (a stimulus to geodynamic considerations): Journal of Geodynamics, v. 34, p. 99–126, doi: 10.1016/S0264-3707(02)00026-1.

Scheepers, P.J.J., and Langereis, C.G., 1994, Paleomagnetic evidence for counter-clockwise rotations in the southern Apennines fold-and-thrust belt during the late Pliocene and middle Pleistocene: Tectonophysics, v. 239, p. 43–59, doi: 10.1016/0040-1951(94)90106-6.

Scheepers, P.J.J., Langereis, C.G., and Hilgen, F., 1993, Counterclockwise rotations in the southern Apennines during the Pleistocene: Paleomagnetic evidence from the Matera area: Tectonophysics, v. 225, p. 379–410, doi: 10.1016/0040-1951(93)90306-5.

Schiano, P., Clocchiatti, R., Ottolini, L., and Busà, T., 2001, Transition of Mount Etna lavas from a mantle-plume to an island-arc magmatic source: Nature, v. 412, p. 900–904, doi: 10.1038/35091056.

Schiano, P., Clocchiatti, R., Ottolini, L., and Sbrana, A., 2004, The relationship between potassic, calc-alkaline and Na-alkaline magmatism in south Italy volcanoes: A melt inclusion approach: Earth and Planetary Science Letters, v. 220, p. 121–137, doi: 10.1016/S0012-821X(04)00048-2.

Scrocca, D., Carminati, E., and Doglioni, C., 2005, Deep structure of the southern Apennines (Italy): Constraints vs. speculations: Tectonics, v. 24, doi: 10.1029/2004TC001634.

Selvaggi, G., and Chiarabba, C., 1995, Seismicity and P-wave velocity image of the southern Tyrrhenian subduction zone: Geophysical Journal International, v. 122, p. 818–826.

Seranne, M., 1999, Early Oligocene stratigraphic turnover on the west Africa continental margin: A signature of the Tertiary greenhouse-to-icehouse transition?: Terra Nova, v. 11, no. 4, p. 135–140, doi: 10.1046/j.1365-3121.1999.00246.x.

Serri, G., Innocenti, F., and Manetti, P., 2001, Magmatism from Mesozoic to Present: Petrogenesis, time-space distribution and geodynamic implications, *in* Vai, G.B., and Martini, I.P., eds., Anatomy of an Orogen: The Apennines and Adjacent Mediterranean Basins: Dordrecht, The Netherlands, Kluwer Academic Publishers, p. 77–104.

Silver, P.G., Russo, R.M., and Lithgow-Bertelloni, C., 1998, Coupling of South American and African plate motion and plate deformation: Science, v. 279, p. 60–63.

Smith, G.P., Wiens, D.A., Fischer, K.M., Dorman, L.M., Webb, S.C., and Hildebrand, J.A., 2001, A complex pattern of mantle flow in the Lau backarc: Science, v. 292, p. 713–716, doi: 10.1126/science.1058763.

Spadini, G., and Podladchikov, Y., 1996, Spacing of consecutive normal faulting in the lithosphere: A dynamic model for rift axis jumping (Tyrrhenian Sea): Earth and Planetary Science Letters, v. 144, p. 21–34, doi: 10.1016/0012-821X(96)00165-3.

Speranza, F., 1999, Paleomagnetism and the Corsica-Sardinia rotation: A short review: Bollettino della Società Geologica Italiana, v. 118, p. 537–543.

Speranza, F., Mattei, M., Sagnotti, L., and Grasso, F., 2000, Rotational differences between the northern and southern Tyrrhenian domains: Paleomagnetic constraints from the Amantea Basin (Calabria, Italy): Journal of the Geological Society of London, v. 157, p. 327–334.

Suhadolc, P., and Panza, G.F., 1989, Physical properties of the lithosphere-asthenosphere system in Europe from geophysical data, *in* Boriani, G., et al., eds., The Lithosphere in Italy: Roma, p. 15–37.

Tatsumi, Y., 1986, Formation of the volcanic front in subduction zones: Geophysical Research Letters, v. 13, p. 717–720.

Thorkelson, D.J., 1996, Subduction of diverging plates and the principles of slab window formation: Tectonophysics, v. 255, p. 47–63, doi: 10.1016/0040-1951(95)00106-9.

Tonarini, S., Armienti, P., D'Orazio, M., and Innocenti, F., 2001, Subduction-like fluids in the genesis of Mt. Etna magmas: Evidence from boron isotopes and fluid mobile elements: Earth and Planetary Science Letters, v. 192, p. 471–483, doi: 10.1016/S0012-821X(01)00487-3.

Tonarini, S., Leeman, W.P., Civetta, L., D'Antonio, M., Ferrara, G., and Necco, A., 2004, B/Nb and δ^{11}B systematics in the Phlegrean volcanic district (PVD): Journal of Volcanology and Geothermal Research, v. 133, p. 123–139, doi: 10.1016/S0377-0273(03)00394-9.

Tovish, A., Schubert, G., and Luyendyk, B.P., 1978, Mantle flow pressure and the angle of subduction: Non-Newtonian corner flows: Journal of Geophysical Research, v. 83, no. B12, p. 5892–5898.

Trua, T., Serri, G., and Marani, M., 2003, Lateral flow of African mantle below the nearby Tyrrhenian plate: Geochemical evidence: Terra Nova, v. 15, no. 6, p. 433–440, doi: 10.1046/j.1365-3121.2003.00509.x.

Turner, S., and Hawkesworth, C.J., 1998, Using geochemistry to map mantle flow beneath the Lau Basin: Geology, v. 26, no. 11, p. 1019–1022, doi: 10.1130/0091-7613(1998)026<1019:UGTMMF>2.3.CO;2.

van der Voo, R., 1993, Paleomagnetism of the Atlantic Tethys and Iapetus Oceans: Cambridge, Cambridge University Press, 411 p.

Verges, J., and Sabat, F., 1999, Constraints on the Neogene Mediterranean kinematic evolution along a 1000 km transect from Iberia to Africa, *in* Durand, B., Mascle, A., Jolivet, L., Horvàth, F., and Séranne, M., eds., The Mediterranean Basins: Tertiary Extension within the Alpine Orogen: Geological Society of London Special Publication 156, p. 63–80.

Wendt, J.I., Regelous, M., Collerson, K.D., and Ewart, A., 1997, Evidence for a contribution from two mantle plumes to island-arc lavas from northern Tonga: Geology, v. 25, no. 7, p. 611–614, doi: 10.1130/0091-7613(1997)025<0611:EFACFT>2.3.CO;2.

Wezel, F.C., Savelli, D., Bellagamba, M., Tramontana, M., and Bartole, R., 1981, Plio-Quaternary depositional style of sedimentary basins along insular Tyrrhenian margins, *in* Wezel, F.C., ed., Sedimentary Basins of Mediterranean Margins: Roma Consiglio Nazionale Ricerche Italian Project of Oceanography, p. 239–269.

Wortel, R., and Spakman, W., 2000, Subduction and slab detachment in the Mediterranean-Carpathian region: Science, v. 290, p. 1910–1917, doi: 10.1126/science.290.5498.1910.

Yogodzinski, G.M., Lees, J.M., Churikova, T.G., Dorendorf, F., Woerner, G., and Volynets, O.N., 2001, Geochemical evidence for the melting of subducting ocean lithosphere at plate edges: Nature, v. 409, p. 500–504, doi: 10.1038/35054039.

Manuscript Accepted by the Society 9 June 2006